ARRIVE ALIVE:

DETECT AND PREDICT LANE DEPARTURES FROM THE STEERING WHEEL SIGNAL

PIA FORSMAN (ED.), MAX SANDSTRÖM, AXI HOLMSTRÖM,
EETU LAMPSIJÄRVI, GÖRAN MACONI, SHABANA AHMADZAI,
EDWARD HÆGGSTRÖM

HELSINGIN YLIOPISTO
HELSINGFORS UNIVERSITET
UNIVERSITY OF HELSINKI

MATEMAATTIS-LUONNONTIETEELLINEN TIEDEKUNTA
MATEMATISK-NATURVETENSKAPLIGA FAKULTETEN
FACULTY OF SCIENCE

ARRIVE ALIVE:

DETECT AND PREDICT LANE DEPARTURES FROM THE STEERING WHEEL SIGNAL

PIA FORSMAN (ED.), MAX SANDSTRÖM, AXI HOLMSTRÖM,
EETU LAMPSIJÄRVI, GÖRAN MACONI, SHABANA AHMADZAI,
EDWARD HÆGGSTRÖM

HELSINGIN YLIOPISTO
HELSINGFORS UNIVERSITET
UNIVERSITY OF HELSINKI

MATEMAATTIS-LUONNONTIETEELLINEN TIEDEKUNTA
MATEMATISK-NATURVETENSKAPLIGA FAKULTETEN
FACULTY OF SCIENCE

University of Helsinki

Faculty of Science

Department of Physics

Gustaf Hällströmin katu 2a

FI-00560 Helsinki

http://www.physics.helsinki.fi/

This publication has been accomplished with the support by The Finnish Work Environment Fund.

ISBN 978-951-51-1860-8 (hardcover)

ISBN 978-951-51-1861-5 (PDF)

Unigrafia, Helsinki 2015

TIIVISTELMÄ

Kolmellakymmenelläneljällä osallistujalla, jotka yhteensä ajoivat 31200 km korkealaatuisissa rekkasimulaattoreissa, näytimme että kaistalta poikkeamisia voi havaita rattisignaalista ja että ajonjälkeiset simulaattoripahoinvointitulokset korreloivat ajoa edeltävän sykevälivaihtelun kanssa.

Työ- ja liikenneturvallisuusvirkailijat ovat kauan tiedostaneet vastatoimien tarpeen väsyneenä ajamiseen, koska se on suuri osatekijä liikenneonnettomuuksissa [1, 2]. Suomessa jopa 40 % kyselyihin vastanneista pitkän matkan rekkakuskeista ja 21 % lyhyen matkan rekkakuskeista, raportoivat vaikeuksia hereillä pysymisessä jopa 20 % matkoistaan. Yli 20 % vastanneista pitkän matkan rekkakuskeista myöntävät nukahtaneensa rattiin ainakin kahdesti [3].

Väsynyt kuljettaja tekee harvoja mutta suuria korjausliikkeitä ratilla [4, 5], mikä kasvattaa ulosajon riskiä [6, 5]. Nykyiset kaistavahdit havaitsevat vain 30-40 % kaikista kaistalta poikkeamisista koska ne ovat video-pohjaisia ja menettävät usein tietoa [8]. Osoitimme äskettäin että auton siirtofunktio mahdollistaa rattisignaalin muuntamisen kaistasijaintisignaaliksi [9]. Kaistavahti, joka perustuisi tähän menetelmään, olisi luotettavampi ja sen pitäisi havaita kaistalta poikkeamiset suuremmalla herkkyydellä kuin nykyiset videopohjaiset järjestelmät.

On epävarmaa, ehkäiseekö kaistavahti todella onnettomuuksia havaitsemalla kaistalta poikkeamisia [8, 10, 11]. Teknologia, joka ennustaisi kaistalta poikkeamisia, antaisi kuljettajalle aikaa ehkäistä lähestyvää vaaratilannetta. Tähän asti tutkijat ovat käyttäneet yhdistelmää autopohjaisista ja fysiologisista signaaleista ennustaakseen väsymystä viisi minuuttia eteenpäin [12]. Toisaalta, järjestelmä joka perustuu fysiologisiin signaaleihin saattaa olla häiritsevä kuljettajalle ja altis tiedon menetykselle. Kvanttineuroverkkoja (QNN) käytetään ennustamaan nopeita ja hetkellisiä vaihteluja osakemarkkinoilla (ihmisen toiminta) ja auringonpilkkujen aktiviteettiä (luonnollinen toiminta) [13-15], ja niitä voisi käyttää myös ennustamaan kaistalta poikkeamisia rattisignaaleista.

Simulaattoripohjainen koulutus on tärkeää ammattikuljettajien koulutuslaitoksille, koska se mahdollistaa vaaratilanteiden emuloinnin ja analysoinnin, kuten esim. miten toimia kun linja-auto ajaa jäisen tiekohdan yli [16]. Vaikka simulaattorit ovat arvokkaita koulutuksen kannalta, kouluttajien pitää varautua opiskelijoihin, jotka kärsivät simulaattoripahoinvoinnista [17]. Simulaattoripahoinvointi aiheuttaa traumoja, jotka rajoittavat koulutuksen tehokkuutta, ja lisää keskeyttämisten määrää [18]. Simulaattoripahoinvoinnille alttiiden opiskelijoiden tunnistaminen antaisi kouluttajalle mahdollisuuden keskeyttää harjoituskerran ennen pahoinvoinnin alkamista – tämä parantaisi pahoinvoinnille alttiiden opiskelijoiden simulaattorikoulutuksen laatua ja määrää. Koska sykevälivaihtelu (HRV) on stressitunniste, sitä voitaisiin käyttää ennustamaan simulaattori-pahoinvointia.

Projektilla (2014-2015) oli kolme tavoitetta: 1) ennustaa simulaattoripahoinvointia, 2) havaita ja 3) ennustaa kaistalta poikkeamisia rattisignaalista. Tutkimukseen värvättiin 34 opiskelijaa Työtehoseuran Logistiikka ja ajoneuvot-osastolta. Koehenkilöt ajoivat Työtehoseuran kahdessa korkealaatuisessa ajosimulaattoreissa 80 km/h nopeudella 55 min joka kolmas tunti 36 tunnin valvomisen ajan yhteensä 31200 km ajoa. Ajokertojen aikana tallensimme simulaattoreiden ratti- ja kaistasijaintisignaaleja 60 Hz:n näytteistystaajuudella. Mittasimme myös osallistujien sydänkäyrää (ECG) 500 Hz:llä. Välittömästi ennen jokaista ajokertaa ja jokaisen ajokerran jälkeen osallistujat tekivät 10-minuutin

valppaustestin (Psychomotor Vigilance Test, PVT) ja arvioivat pahoinvoinnin, okulomotorisen epämukavuuden ja disorientaation oireet simulaattoripahoinvointi-kyselyssä (Simulator Sickness Questionnaire, SSQ) samalla, kun sydänkäyrää mitattiin.

Käytimme ensimmäisinä kvantitatiivista sydänkäyrää ennustamaan mitkä osallistujat tulevat kokemaan simulaattoripahoinvointia, ja keskityimme dataan kolmen ensimmäisen ajokerran ajalta, jolloin koehenkilöt vielä olivat virkeitä (välttääksemme väsymyksen vaikutuksen heidän SSQ-arvoihinsa). N=15 osallistujalla SSQ-tulos oli ajokertojen jälkeen korkeampi kuin ennen ajoja, ja muilla n=19 ei. Ennen ajoa (PVT- ja SSQ tehtävien aikana) LF/HF-suhde (joka on ECG-signaalista laskettu tunnusluku [30]) oli pienempi niillä osallistujilla, jotka saivat korkeamman SSQ-arvon ajon jälkeen. Vaikka ero kahden ryhmän välillä (n=15 ja n=19) ei ollut tilastollisesti merkitsevä, tämä ero osoittaa että LF/HF-suhteesta voisi ennustaa simulaattoripahoinvointia. Perustelu tälle on se, että kukaan osallistujista ei saanut korkeita SSQ-arvoja ensimmäisten kolmen testikerran aikana – LF/HF-suhtessa havaittu ero n=15 kuljettajalla oli lievä (toisin sanoen, kukaan kuljettajista ei keskeyttänyt ajoa simulaattoripahoinvoinnin takia). Seuraavaksi meidän pitäisi validoida parametri vapaaehtoisilla, jotka kokevat simulaattoripahoinvointia. Se, että kukaan osallistujista ei saanut korkeita SSQ-arvoja levänneenä tarkoittaa myös, että ammattikuljettajien koulutuslaitokset voisivat käyttää koejärjestelyjämme helpottaakseen opiskelijoidensa totuttautumista simulaattoripohjaiseen koulutukseen. Eritoten, koulutuksen aloittaminen maantieajoskenaariolla auttaisi opiskelijoita sopeutumaan simuloituun ympäristöön.

Havaitaksemme kaistalta poikkeamisia rattisignaalista määritimme ensin simulaattoreiden siirtofunktiot ja käytimme niitä laskemaan kaistasijaintia mitatuista rattisignaaleista. Pearsonin korrelaatiokerroin laskettujen ja mitattujen kaistasijaintisignaalien välillä oli r=0.48 (n=3151). Tämä vastaa aikaisempia tutkimustuloksia (Työsuojelurahaston projekti #109257). Seuraavaksi kehitimme algoritmin, joka käytti laskettuja kaistasijaintisignaaleja varoittaakseen kaistalta poikkeamisista kolme sekuntia etuajassa. Herkkyys oli 47 % ja tarkkuus oli 71 %. Korrelaatio laskettujen ja mitattujen kaistasijaintisignaalien välillä oli pienempi kuin aikaisemmassa tutkimuksessamme ($r\geq$0.78 [9]), mutta herkkyys kehittämällemme kaistavahtialgoritmille oli suurempi kuin nykyisten video-pohjaisten kaistavahtien saavuttama 40 % herkkyys. Yhteenvetona tämä tarkoittaa sitä, että tuotimme ensimmäiset tieteelliset todisteet sille, että kaistalta poikkeamisia voidaan havaita rattisignaalista. Seuraavaksi meidän tulisi kokeilla, onko ehdotettu menetelmä kenttäkelpoinen.

Ennustaaksemme kaistalta poikkeamisia rattisignaalista koulutimme ensin yhden QNN:n kahdella piilotetulla kerroksella ennustamaan rattisignaalia eteenpäin yhdellä aikapisteellä. Koska alinäytteistimme rattisignaalia 10 Hz:iin QNN ennusti 0,1 s eteenpäin. Seuraavaksi käytimme ennustettua signaalia kaistasijainnin laskemiseen siirtofunktiolla – korrelaatio lasketun ja mitatun kaistasijaintisignaalin välillä oli r=0.73 (n=1). Yhteenlaskettuna näytimme ensimmäiset tieteelliset todisteet sille, että QNN:illä voidaan ennustaa kaistasijaintisignaalia. Seuraava tehtävämme on kasvattaa ennustushorisonttia.

Yhteenveto:
1) Tuotimme ensimmäinen näyttö, että suhteellisen matala LF/HF suhde edeltää pientä kasvua SSQ-tuloksissa. Tämä tulos perustuu koehenkilöryhmään missä selväpiirteistä simulaattori-pahoinvointia ei esiintynyt. Ennen kuin voimme tehdä johtopäätöksiä, meidän tulisi validoida tulokset vapaaehtoisilla jotka selvästi potevat simulaattoripahoinvointia.

2) Kehitimme myös algoritmin joka havaitsee kaistalta poikkeamisia rattisignaalista suuremmalla herkkyydellä kuin nykyiset video-pohjaiset kaistavahdit (47 % vs. 40 %).

Seuraava tehtävämme on lisätä menetelmän herkkyyttä. Koska menetelmä kehitettiin laboratorio-olosuhteissa, meidän tulisi validoida sen kenttäkelpoisuus. Tällöin olemme varustaneet tieliikenteen ensimmäisellä luotettavalla autopohjaisella kaistavahdilla.

3) Lopuksi osoitimme, että QNN pystyy ennustamaan rattisignaalia 0,1 s eteenpäin 0,7 % virheellä (eli isolla tarkkuudella), ja että ennustettua signaalia voidaan käyttää laskemaan kaistasijaintia. Jos pystymme kasvattamaan ennustushorisonttia, meillä on tarvittavat osatekijät ennustavalle kaistavahdille.

SUMMARY

With 34 participants that collectively drove 31200 km in high-fidelity truck simulators, we showed that one can detect lane departures from the steering wheel signal, and that post-drive simulator sickness scores correlate with pre-drive heart rate variability data.

Work- and traffic safety officials have long acknowledged the need for countermeasures against drowsy driving, a main contributor to road crashes [1, 2]. In Finland, even 40% of polled long-haul truck drivers and 21% of polled short-haul truck drivers report difficulties staying awake during 20% of their journeys. More than 20% of the polled long-haul drivers admit to nodding off at the wheel at least twice [3].

A drowsy driver makes less frequent but large corrective steering wheel movements [4, 5], which increases the risk for running off the road [6, 7]. So far, current in-car lane departure warning (LDW) systems only recognize 30-40% of all imminent lane departures, because they are video-based and often loose data [8]. We recently showed that the car's transfer function provides a way to transform the steering wheel signal into a lane position signal [9]. An LDW system that relies on this approach would be more robust and should detect lane departures with higher sensitivity than the current video-based systems do.

Whether an LDW system truly prevents accidents by detecting lane departures is unknown [8, 10, 11]. A technology that predicts lane departures would give the driver time to safely counteract an upcoming event. So far researchers have used a combination of car-based and physiological signals continuously recorded while driving to predict drowsiness even five minutes in advance [12]. However, a system that relies on physiological metrics may be obtrusive and prone to data loss. Quantum Neural Networks (QNN) are used to predict e.g. transient fluctuations in the stock market (human action) and sunspot activity (natural action) [13-15], and may also be used to predict lane departures from the steering wheel signal.

For institutions that train professional drivers, simulator-based training is important because it allows emulating and analyzing dangerous situations, like e.g. what to do when the bus hits an icy spot [16]. While simulators are valuable for education, instructors must be prepared for students who suffer from simulator sickness [17]. It leaves a stigma which limits the effectiveness of training and increases the student dropout rate [18]. Catching a student prone to simulator sickness would enable the instructor to end the training session before the student experiences simulator sickness – for susceptible students this reflects positively on training quality and quantity. As heart rate variability (HRV) is a marker of stress, it could be used to predict simulator sickness.

The project (2014-2015) had three aims: 1) to predict simulator sickness and to 2) detect and 3) predict lane departures from the steering wheel signal. We enrolled 34 students at Työtehoseura's branch of logistics and vehicles. They drove in Työtehoseura's two high-fidelity driving simulators at 80 km/h for 55 minutes every third hour during 36 hours of sustained wakefulness – collectively covering 31200 km of driving. During the driving sessions we logged the simulators' steering wheel and lane position signals at 60 Hz. We also recorded the participants' electrocardiogram (ECG) at 500 Hz. Immediately before and after each driving session the participants took a 10-minute Psychomotor Vigilance Test (PVT) and rated their symptoms of nausea, oculomotor discomfort, and disorientation on the Simulator Sickness Questionnaire (SSQ) while we recorded their ECG.

We are the first to try to use quantitative ECG to predict which participants will experience simulator sickness, and we focused on data that was recorded during the first three test sessions when they still were rested (to avoid that sleepiness confounded their SSQ-ratings). *N*=15 participants scored higher on the SSQ after the drives, whereas the other *n*=19 participants did not. During the pre-drive PVT and SSQ tests, the ratio of the low- and high frequency components in the ECG signal (LF/HF ratio) [30] was lower in the participants who scored higher on the SSQ after the drive. While the difference between the two groups (*n*=15 and *n*=19) was not statistically significant, it indicates that the LF/HF ratio may be a potent predictor of simulator sickness. The rationale is that overall, none of the participants scored high on the SSQ during the first three test sessions – the effect that the LF/HF ratio detected in the *n*=15 drivers was mild (i.e. none of them stopped driving because of simulator sickness). Next, we should validate the parameter with volunteers who express simulator sickness and develop a user-friendly interface for the instructor. The fact that none of the participants scored high on the SSQ when they were rested also means that institutions that train professional drivers could use our set-up to ease their students into simulator-based training. Specifically, starting the training in a highway scenario would help the student adapt to the simulated environment.

To detect lane departures from the steering wheel signal, we first determined the simulators' transfer functions and used them to derive the lane position signals from the recorded steering wheel signals. The Pearson correlation between the derived and recorded lane position signals was r=0.48 (n=3151). This is in line with our previous findings (Finnish Work Environment Fund project #109257). Next, we developed an algorithm that used the derived lane position signal to warn about lane departures up to three seconds in advance. The sensitivity was 47% and the specificity was 71%. The correlation between the derived and recorded lane position signals was lower than in our previous research ($r \geq 0.78$ [9]), but the sensitivity of the new LDW algorithm was higher than the sensitivity that the current video-based LDW systems achieve (40%). Taken together this means that we showed the first scientific proof that lane departures can be detected from the steering wheel signal. Next, we should test whether the proposed system is field-capable.

To predict lane departures from the steering wheel signal, we first trained a QNN with two hidden layers to predict the steering wheel signal one data point ahead. Because we down sampled the steering wheel signal to 10 Hz the QNN predicted 0.1 s ahead. Next, we used the predicted signal to derive the lane position signal with the transfer function approach – the correlation between derived and measured lane position signals was r=0.73 (n=1). Taken together we showed the first scientific proof that QNNs can predict the lane position signal. Our next task is to increase the prediction horizon.

In conclusion:
1) We showed the first results that a low pre-drive LF/HF ratio correlates with a small post-drive increase in SSQ scores. This finding was based on a group of people with no pronounced simulator sickness, so before any firm conclusions can be drawn, we need to replicate the results with volunteers who clearly express simulator sickness.

2) We developed an algorithm that detects lane departures from the steering wheel signal with higher sensitivity than the current video-based systems do. Our next task is to increase the sensitivity. Because the method was developed from data recorded in a laboratory-environment we also need to test whether it works in the field. If it does, we have provided road transportation with the first LDW system that is based on a robust car-based signal.

3) Finally, we showed that QNNs can predict the steering wheel angle 0.1 s ahead with 0.7% error (i.e., high accuracy) and that the predicted signal can be used to derive the lane position signal. If we can increase the prediction horizon we have the necessary elements for a predictive car-based LDW system.

Table of Contents

1 AIMS

Our long-term goal is to develop sensor-and-signal-processing technology that detects and predicts drowsiness-related lane departures from the steering wheel signal with high sensitivity and specificity. This would be a robust and unobtrusive technology that would give the driver time to anticipate and safely counteract upcoming events and to avoid an accident. We also develop a signal-processing technology to predict the onset of simulator sickness. This would give the instructor time to end a training session before the student experiences simulator sickness symptoms.

Our specific study aims to test our hypotheses and meet our overall aim were:

Aim 1: To predict simulator sickness while driving in a high-fidelity driving simulator.

Rationale 1: Heart rate variability (HRV) is a marker of stress and we expect that simulator sickness decreases HRV.

Deliverable 1: We identified a quantitative tool that predicts simulator sickness, and we determined how much in advance it can predict the onset.

Success criteria 1: The tool predicts onset of simulator sickness before the driver perceives the symptoms (which usually occurs during the first 30 minutes if the driver is susceptible [18]).

Aim 2: To detect drowsiness-related lane departures from the simulator's steering wheel.

Rationale 2: The transfer function (TF) approach suffers no data loss due to invisible lane markers. It provides lane-related metrics of driving performance from the steering wheel signal.

Deliverable 2: Quantitative algorithm that reliably *detects drowsiness-related lane departures in a non-invasive manner*. Knowledge whether the TF-approach is a feasible starting point for a non-video-based lane departure warning system.

Success criteria 2: The Pearson correlation between the calculated and recorded lane position is $r \geq 0.78$ [9]. The sensitivity of the detection algorithm is 40% [8].

Aim 3: To predict drowsiness-related lane departure from the simulator's steering wheel signal with Quantum Neural Networks (QNNs).

Rationale 3: QNNs can predict transient fluctuations in real life (stock market and sunspot activity).

Deliverable 3: Mathematical model *predicting drowsiness-related lane departure from the steering movements that the individual driver makes*.

Success criteria 3: The sensitivity of the prediction model is 40% [8].

2 MATERIALS AND METHODS

2.1 Participants

N=34 students at Työtehoseura's branch of logistics and vehicles participated in our study (Table 1). The inclusion criteria were: good health (by questionnaire); good sleep (by questionnaire, actigraphy, sleep diary); ability to abstain from caffeine for 37 hours; body mass index between 22–30; and no medication affecting sleep or sleepiness. The participants arrived and departed from the test site by taxi. They gave their written informed consent, and we compensated them for their time. The University of Helsinki Institutional Review Board approved the study in June 2013.

Table 1. Participants during the weeks 37-43.

Condition [a]	**N** (count)	**Age** (mean ± SD, range)
Night [b]	16	30 ± 12 (18-55)
Day [c]	18	34 ± 11 (19-52)
	34	32 ± 12 (18-55)

[a] The condition was either driving all sessions in night-time scenarios or in scenarios with clear daylight

[b] All drivers were men: one aborted after 21 hours into the experiment, another after 24 hours.

[c] All but two drivers were men: one aborted after 24 hours into the experiment, another after 27 hours.

2.2 Protocol

On Monday the participants took a test session to familiarize themselves with the procedures (Table 2). We asked them to arrive rested to the sleep deprivation experiment on Friday morning. Therefore, we required ten hours time in bed per night (21:00-7:00, Mon-Fri), which we checked with at-home sleep diaries and wrist-worn actigraphs.

On Friday, the participants woke up at 6:00 and arrived at the test site by 7:30. We checked their compliance with our sleep-requirements and then we served them breakfast. At 8:45 the first test session started (Table 2). The sessions repeated every third hour until 19:15 on Saturday when the participants left for recovery sleep at home.

Smokers (N=12) could have a cigarette immediately after a session (in a ventilated room at the test site). During the experiment we served 12 standardized meals (averaging 275 kcal, totaling 2200 kcal/24 hours) immediately after each session. No caffeine was allowed. Between the sessions the participants had 90 minutes "own time" during which they could read, play cards and board games, watch movies, and converse with each other in the common room. The light level in the common room was 52 ± 4 lux and the temperature was 23 ± 1 °C. An experimenter monitored the participants continuously to ensure that they stayed awake.

Työtehoseura has two high-fidelity driving simulators. Therefore each study run could accommodate six participants and therefore we shifted the experimental protocol by one hour for participants 3-4 (wake up at 7:00 on Fri) and by two hours for participants 5-6 (wake up at 8:00 on Fri).

Table 2. Experimental protocol progressing from left to right. Rows represent a measurement (see section 2.3). Between 8:45 on Friday and 19:15 on Saturday we recorded electrocardiogram (ECG) nonstop. Starting 9:00 on Friday, we administered a 55-minute driving session every third hour. During each driving session we recorded the drivers' eye lid movements (E). Fifteen minutes before a driving session we recorded the Karolinska Sleepiness Scale (KSS), administered a 10-minute psychomotor vigilance test (PVT), and recorded the simulator sickness questionnaire (SQQ). Immediately after a driving session we recorded SSQ, KSS, PVT.

Test session			**1**			**2**			**…**	**12**		
Time of day	**6**	**7**	**8**	**9**	**10**	**11**	**12**	**13**		**17**	**18**	**19**
Hours in study	**0**	**1**	**2**	**3**	**4**	**5**	**6**	**7**		**35**	**36**	**37**
Driving+E				*			*				*	
KSS+PVT+SSQ			*		*	*		*		*		*
ECG			*	*	*	*	*	*		*	*	*

2.3 Measurements

Each test session included a computerized version of the Karolinska Sleepiness Scale (KSS, [19]); a 10-min Psychomotor Vigilance Test (PVT, [20]); a computerized version of the Simulator Sickness Questionnaire (SSQ, [21]); a 55-min driving session on Työtehoseura's high-fidelity driving simulator; another SSQ, KSS, and PVT. Thus, each driving session was preceded and followed by a battery of independent, established indices of fatigue [22]. During each driving session we recorded the driver's eyelid movements and 2-lead electrocardiogram (ECG).

2.3.1 Subjective sleepiness, objective sleepiness, and simulator sickness

As an independent measure of subjective fatigue, we used the Karolinska Sleepiness Scale (KSS), where the participant rates the feeling of sleepiness during the last 5 minutes from 1 (very alert) to 9 (very sleepy) [19].

As an independent measure of objective fatigue, we used the Psychomotor Vigilance Test (PVT). The PVT is a simple reaction time task with high stimulus density, which measures sustained attention [20]. The primary outcome metric is the number of lapses, defined as reaction times exceeding 500 ms.

As an independent measure of subjective simulator sickness, we used the Simulator Sickness Questionnaire (SSQ), where the participant rates 16 symptoms related to nausea, oculomotor disturbances, and disorientation on a 4-point scale from 0 to 3. The primary outcome metric is the total score [21]:

$$TS = N \times 9.58 + O \times 7.58 + D \times 13.92 \times 3.74, \quad (1)$$

where N, O, and D are the marks on the nausea, oculomotor, and disorientation scales.

2.3.2 Driving

During every driving session, the participants drove a simulated truck in a fixed-base, high-fidelity driving simulator (Fig. 1). The simulator employs hardware and software to realistically simulate the mechanics and driving characteristics of a real truck.

The simulator sampled steering wheel angle θ, lateral lane position x, vehicle pitch φ, and driving speed v at a variable rate above 80 Hz, depending on the amount of computation required to produce the simulated scenery at a given moment. A separate computer with the software RTMaps (Intempora) logged time stamps and data from the simulator (Fig. 2). Offline we down sampled the signals to 60 Hz.

The simulated driving track comprised a network resembling Finnish uneventful rural roads with no other traffic (Fig. 3). Because each driver completed 12 driving sessions, we defined 12 combinations of starting points and driving directions along the track and randomized their order to the driving sessions.

The first 16 participants drove all 12 sessions in a nighttime scenario where the average illuminance at the drivers' eye level was 0.9 lux (simulator 1) and 1.4 lux (simulator 2). The next 18 participants drove all sessions in daylight clear view where the average illuminance at the drivers' eye level was 3.0 lux (simulator 1) and 4.9 lux (simulator 2). The road condition on the road was full friction. We instructed all participants to keep the posted speed limit 80 km/h, stay in the lane, and keep their hands on the steering wheel, while keeping the cruise control and radio off.

Our database covers 374 hours and 31200 km of driving (34 drivers, 12 driving sessions, 55 min/session, approximately 80 km/hour). Along the 110 km track there were 21 straightaways that were 400 m or longer totaling 31 km (Fig. 3).

Fig 1. The simulator comprised parts of a real truck. The scenery was projected on screens covering the wind shields (SIMRAK, Tampere).

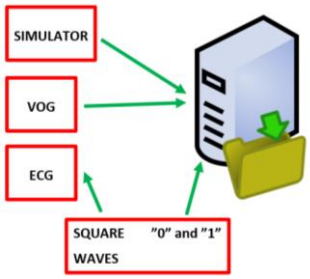

Fig 2. Computer time stamps incoming signals from the attached devices. ECG is electro-cardiogram (section 2.3.3) and VOG is video-oculography (section 2.3.4)

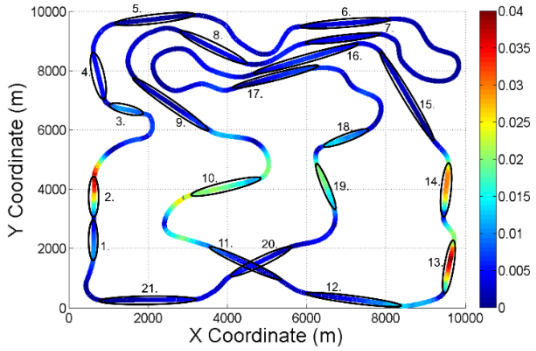

Fig 3. Map of the 110 km simulated driving track. Colour indicates m/20 m (red means incline). The black numbered ovals show 21 straightaways that were longer than 400 m.

2.3.3 Electrocardiograms

During every driving session, we recorded the participants' 2-lead ECG with eMotion Faros 180° (Mega Electronics Ltd) and Ambu® BlueSensor VL electrodes (Ambu A/S) at 500 Hz.

Before the first driving session, we cleaned the skin area over the collarbone and at the end of the ribcage with ethanol wet wipes and attached the electrodes according to the device manufacturer's instructions. We checked the signal quality by visual inspection (the device worked in online Bluetooth mode). If the R-peaks in the QRS-complexes were difficult to recognize, we replaced the electrodes. Otherwise we set the device to data logging mode.

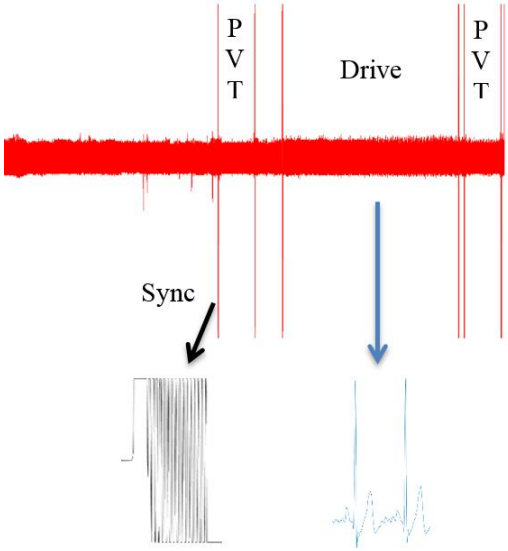

Fig. 4. Measured ECG signal with synchronization signals (the zoom shows QRS complexes).

We did not remove the electrodes during the sleep deprivation experiment, unless we found problems with electrode adhesion or signal quality.

To allow post-hoc synchronization of the recorded ECG-signals with the recorded driving data, we connected a customized device to the computer that ran the RTMaps software and that logged the time stamps and data from the driving simulator (Fig. 2). Before a participant climbed into the simulator, we disconnected the eMotion Faros 180° from the electrodes and connec ted it to the customized device via an USB cable the device used a development board, Arduino UNO R3, Arduino Mega). The cus-

tomized device sent a “0” to RTMaps, a 5 V square wave signal to the eMotion Faros 180°, and a “0” to RTMaps. Then we reattached the eMotion Faros 180° to the participant’s electrodes. We repeated the procedure after the driving session (Fig. 4). *Post hoc* we matched the signal that the eMotion Faros 180° recorded and the time stamps of the serial transmissions that the RTMaps recorded. Figure 4 shows an example of recorded ECG and square wave synchronization signal data.

2.3.4 Eyelid movements

During every driving session, we recorded the driver’s eyelid movements at 120 Hz with a video-oculography (VOG) system (AntiSleep, SmartEye Ab). We mounted the system on the dashboard in front of the driver (Fig. 5). The system tracks facial features with an infrared camera and two infrared light sources set in a specific geometry. This eliminates the effect of external light sources on the image. To allow *post hoc* synchronization of the recorded VOG signals with the recorded driving data, we connected the computer running the VOG system to the computer that ran the RTMaps software and that logged the time stamps and data from the driving simulator (Fig. 2). The VOG data was sent on-line to the RTMaps computer.

Fig. 5. AntiSleep camera on the dashboard. Depending on the height of the driver, the camera was 20-40 cm below eye level, angled upward towards the driver's face.

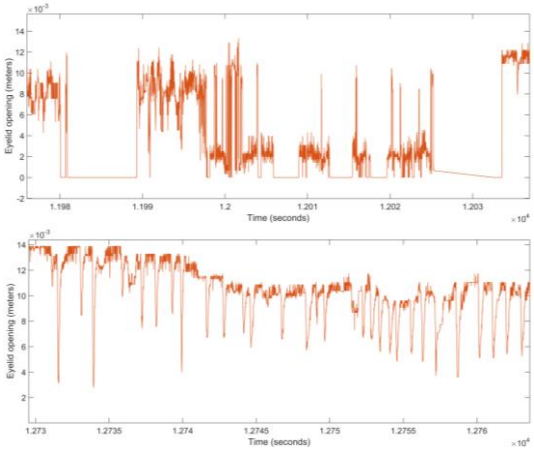

Fig. 6. Good quality eye tracking data (upper) and bad quality eye tracking data (lower).

Immediately before a driver commenced a driving session, we manually adjusted the camera elevation, focus, and aperture. Then we established a facial profile for him/her during a short (~1 min) training session. This optimized the computer vision algorithm, which calculated e.g. head position, head rotation, eye positions, eyelid openings, and gaze direction from the image data that the camera recorded. The computer vision algorithm also estimated the signal quality of each of the calculated metrics on a relative scale from zero to one.

2.3.4.1 Data quality control

Figure 6 shows examples of eye tracking data where the signal quality was high and low. Low signal quality probably stem med from moments when the driver looked away from the camera, negotiated a curve, or e.g. rubbed his/her eyes. To generate high signal quality the computer vision algorithm needs the face to be clearly visible and in the “cor-rect” angle. For the purpose of further data analysis we developed an algorithm that identified signal por-tions with high signal quality according to the following criteria:

1. VOG-signal recorded on a straightaway.
2. Quality of eyelid opening and gaze direction > 0 (provided the AntiSleep software).
3. Estimated quality of head orientation > 0.2 (provided by AntiSleep software).

These requirements excluded 60% of the VOG data from further analysis, but this did not skew the results with respect to drivers or sleep deprivation (by manual inspection).

2.4 Analysis

2.4.1 Subjective sleepiness, objective sleepiness, and simulator sickness

To evaluate the effects of light, time awake, and time on task on the drivers' subjective and objective sleepiness as well as on their symptoms of simulator sickness, we performed mixed-effects analysis of variance (ANOVA) with conditions (night-time vs. daytime), sessions (1 to 12), and pre/post drive measurement as fixed effects, and participants as random effect on the intercept. For our analyses we used IBM SPSS Statistics 23.

2.4.2 Predicting simulator sickness from heart rate variability (Aim 1)

We used cross correlation to locate the synchronization signals in the ECG signal (Fig. 4). We excluded ECG signals that lacked synchronization signals from further analysis (signals from 15 test sessions). We aligned the ECG signals with the simulator data (using the synchronization timestamps that RTMaps recorded). We used Kubios HRV [29] to detect R-peaks in the raw ECG signals and to quantify RR-interval time series (Fig. 7).

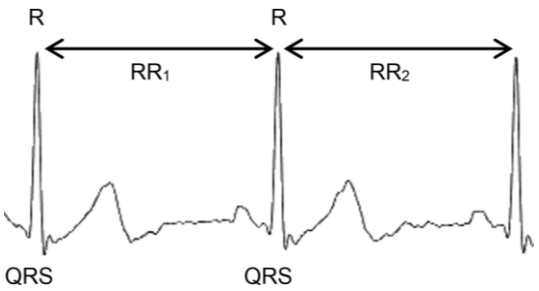

Fig. 7. RR-intervals are the timespans between consecutive R-peaks in the ECG signal.

When we analyzed HRV during driving, we used data where the driving speed $v >$ 50 km/h (including straightaways and curves). When we analyzed HRV during the pre- and post drive PVT+KSS+SSQ sessions, we used data between the synchronizations made on the "PVT" computer (Fig. 4). The selected signals were divided into 5 minute epochs with 99% overlap. For each epoch we computed several HRV parameters (defined in [30]:Mean RR interval, SDNN (Standard deviation of RR-intervals), RMSSD, and pNN50. After linearly detrending the RR-intervals we estimated the power spectral density (PSD) using the Lomb-Scargle periodogram method and computed the HRV parameters: VLF power, LF power, HF power, and LF/HF power ratio by integrating the PSD across each frequency band. Finally, we averaged each parameter across the data recorded in the pre-drive PVT+KSS+SSQ session, the driving session, and the post-drive SSQ+KSS+PVT sessions. For our computations we used MATLAB R2014b.

To evaluate whether the HRV parameters predicted simulator sickness, we only considered data recorded during the first three driving sessions. The rationale is that sleepiness is a confounder in simulator sickness, and until the third driving session the drivers were not affected by sleepiness (Fig. 14). Next, we identified drivers whose SSQ total score had increased form the pre-drive session to the post-drive session (n=15). The rest of the drivers comprised the control group (n=19). We used a two-tailed Student's t-test to evaluate whether the two groups differed from each other during the pre-drive sessions.

2.4.3 Driving

Along the 110 km track there were 21 straightaways that were 400 m or longer, totaling 31 km (Fig. 3). In our analyses of driving performance we used the signals recorded while driving on these straightaways.

2.4.3.1 Deriving lane position from steering (Aim 2)

To derive the lane position signal from the steering wheel signal we assumed that the simulated truck represented a linear time-invariant system and that it moved with constant speed. Then, in frequency space, the transfer function (TF) between the Laplace transforms of the steering wheel angle $\theta(t)$ and the lateral lane position signal $x(t)$ is:

$$TF_m = \frac{P_n(s)}{Q_m(s)}, \quad (2)$$

where P_n and Q_m are polynomials of s with the degree n and m. Let vector $\boldsymbol{C}$ be the (n+1)+(m+1) coefficients of both P and Q, where m is the model order (i.e., degree of the denominator polynomial). We determined the coefficients $\boldsymbol{C}$ separately for model orders 1 to 20. We used Matlab's system identification toolbox to determine the coefficients. Briefly, the toolbox uses the instrument variable method [23] to initialize an estimation of the coefficients, and the Gauss-Newton algorithm [24] to update the estimate. We set the algorithm to repeat the update ten times or until the least-squares error between the current update and the next iteration was 0.01%. We used the training set data (section 3.4.3.4) to derive the $TF_m(s)$, $m\epsilon\{1, \ldots, 20\}$ separately for the two simulators.

Equation 2 assumes that the system output is zero at time zero. However, this is not true in any of our simulations (it would mean that the vehicle was precisely in the center of the lane without weaving). Therefore, TF_m had to be multiplied by $F_m(s)$, which represents the initial conditions. We estimated $F_m(s)$ using Newton's method. With the initial condition at hand, we derived a simulated lane position signal $\hat{x}_m(t)$ from the Laplace transform of the steering wheel angle $\theta(t)$:

$$\hat{x}_m(t) = \mathfrak{L}^{-1}\{X(s)\}(t) = \mathfrak{L}^{-1}\{\Theta(s)TF_m(s)F_m(s)\} \quad (3)$$

We used a validation set to determine which model order m (between 1 and 20) produced the best lane position signal (i.e., the highest correlation between the derived and measured lane position signals). The validation set comprised one randomly chosen driving session in the test data. The validation set comprised steering- and lane position signals from 19 straightaways covering 29 km. We then computed the Pearson correlation between the derived lane position signal (eq. 3) of the m:th order and the lane position signal that the simulator recorded (i.e., our gold standard). We chose the model order with the highest correlation.

2.4.3.2 Detecting lane departure from steering (Aim 2)

To detect lane departures from the steering wheel signal we needed an indicator of lane departures. We computed a driver's preferred position in the lane, y_0, by averaging the lane position during the first 5 minutes of driving, when the driving speed v exceeded 60 km/h:

$$y_0 = \frac{\sum_{t=t_0}^{t_0+N} y(t)}{N+1}, \quad (4)$$

with t_0 such that $v(t)$>60km/h, given $t>t_0$, and N=18000. The lane was 3.5 m wide and the simulated truck was 2.5 m wide. This gave the driver 0.5 m leeway on each side of the vehicle (assuming that the truck was exactly in the middle of the lane). This implies that an average deviation of 0.2 meters from y_0 for a time period t_0 is a suitable indicator of an upcoming lane departure. We computed:

$$y_{LD}(t) = \frac{\sum_{i=t-t_0}^{t} y(i)}{t_0}, \quad (5)$$

and if:

$$|y_0 - y_{LD}| > 0.2\ m, \quad (6)$$

it indicated a lane departure. To identify the optimal time period t_0, we estimated y_{LD} (eq. 5) for different time periods t_0 = {1,2,3,4,5} sec and applied it to our lane departure detection algorithm (eq. 5). We chose the t_0 that rendered the highest sensitivity and specificity. We used the test set data (section 2.4.3.4) to detect lane departures from the steering wheel signal (eqs. 3, 5, 6). To evaluate how many of the actual lane departures our

method detected, we used the following criterion: the algorithm warns about an upcoming lane departure al least three seconds before a true departure (section 2.4.3.3) happens.

2.4.3.3 True lane departures (gold standard)

To validate our method (eq. 6) we needed to identify the lane departures from the lane position signal that the simulator recorded (i.e., our gold standard). We defined lane departures as events where any part of the vehicle was outside the lane markings in the middle or on the right-hand side of the road [28]. We calculated the positon $x_i(t)$ of each corner i of the vehicle at time t:

$$
\begin{aligned}
x_{front\ right}(t) &= x(t) + \frac{w}{2}\cos\varphi, \\
x_{front\ left}(t) &= x(t) - \frac{w}{2}\cos\varphi, \\
x_{back\ right}(t) &= x(t) + l\sin\varphi, \\
x_{back\ left}(t) &= x(t) - l\sin\varphi,
\end{aligned}
\qquad (7)
$$

where x is the position in the lane of the center of the front of the truck in meters, φ is the yaw pitch of the truck in degrees, l is the length of the vehicle (meters), and w is the width of the vehicle (meters) (Fig. 8). Finally, we identified a lane departure if:

$$
\begin{aligned}
&x_i(t) < -1.75 \text{ or } x_i(t) > 1.75 \text{ , while} \\
&x_i(t\text{-}1) > -1.75 \text{ and } x_i(t\text{-}1) < 1.75
\end{aligned}
\qquad (8)
$$

where i represents the four corners of the vehicle in eq. 7 (Fig. 8). Figure 9 shows the number of lane departures.

2.4.3.4 Training and test sets

As training set we used the driving data recorded on the straightaways during the fourth driving session. The rationale for this choice was that on average, the drivers exhibited the least number of lane departures in this session (Fig. 9). As test set we used the driving data recorded on the straightaways during the rest of the driving sessions. Hence, the training set comprised 1000 km of driving (34 drivers, 1 driving session, 31 km) whereas the test set comprised 12000 km of driving (34 drivers, 11 driving sessions, 31 km).

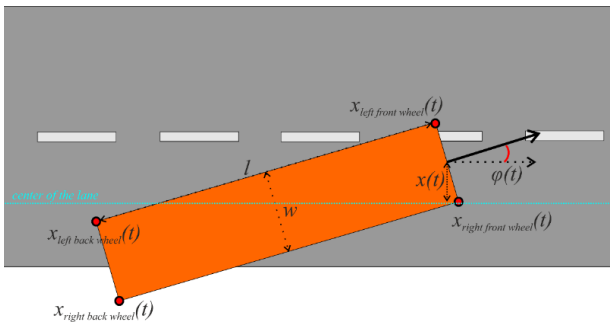

Fig. 8. Variables used to calculate lane departures.

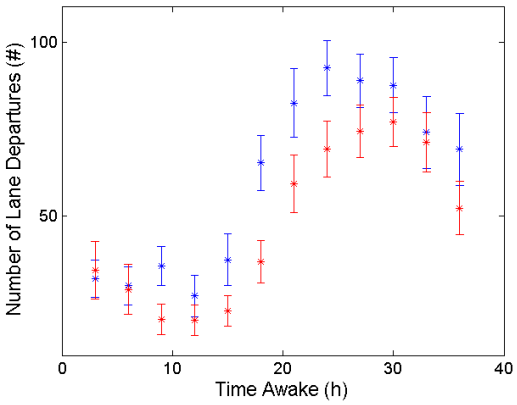

Fig. 9. Number of lane departures for drivers in the night-time (blue circles) and daytime (red circles) driving scenarios as a function of time awake. Mean ± SEM.

2.4.3.5 Quantum Neural Networks (Aim 3)

We used a *time delayed feed-forward* Quantum Neural Network (QNNs, e.g. [25]) to predict steering wheel movements from the steering wheel signal and then we used the predicted signal to derive the lane position signal (section 2.4.3.1). A qubit neuron (Fig. 10) can perform quantum operations like superposition and interference. It has input nodes to which information is fed, and an output node which gives out a value between 0 and 1.

When qubit neurons are combined into networks (Fig. 11) they can perform complicated functions like prediction. To train the network, we fed data from a training set to the network inputs, compared the network output to the desired output, and updated the neural parameters so that the output matched the desired output. In a *feed-forward* network all neurons feed information to the next layer and there is no feedback. In a time delayed network the inputs to one neuron in the input layer is a data point from the preceeding time step.Our QNN had an input layer with 15 qubit neurons, one hidden layer with 40 qubit neurons, another hidden layer with 20 qubit neurons, and an output layer with one neuron (Fig. 11). The number of neurons in the hidden layers were chosen based on the fact that a greater number of neurons in a hidden layer allows more complexity, and therefore possibly smaller errors, but at the cost of longer computing times especially during training. In the first hidden layer we wanted at least twice as many neurons as in the input layer, and since the output layer had only one neuron, the second hidden layer detected general features from the first hidden layer and then grouped them to improve the efficiency of the output neuron.

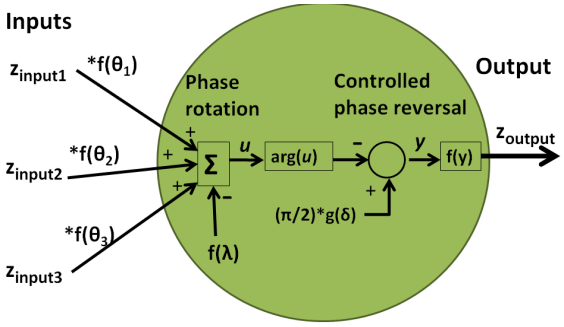

Fig. 10. A qubit neuron in the hidden or output layer. The inputs to the qubit neuron are outputs from the previous layer. The qubit neuron performs phase rotation (eq. 11), controlled phase reversal (eq. 12), and conversion back to a phase state (eq. 13).

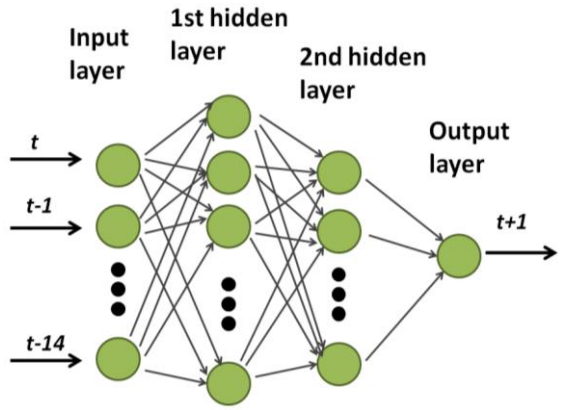

Fig. 11. A Quantum Neural Network combines several qubit neurons. The steering wheel signal's data points from the current time *t* and 14 previous time steps *t-1, t-2, ...t-14* are fed to 15 qubit neurons in the input layer. The output layer has one neuron that predicts the steering wheel signal at time step *t+1*.

We scaled the steering wheel signal to the interval [0,1], which is required for the input layer neurons. The steering wheel movements on straightaways were very small (approximately [-0.01, 0.01]), so before feeding the signal to the QNN we multiplied it by 20 and then added 0.5. This scaling introduced no relative differences between the signals.

Neurons in the input layer converted the steering wheel signal into quantum states with a phase value φ in the range [0, π/2]:

$$z_{input} = f\left(\frac{\pi}{2} \cdot input\right), \tag{9}$$

where the mapping function *f* was:

$$f(x) = e^{ix} \tag{10}$$

Outputs *z* from each input layer neuron *k* was then fed as an input to each neuron in the first hidden layer (Fig. 10). Hidden layer neurons first performed a phase rotation:

$$u = \sum_{k}^{K} \mathrm{z_{input,k}} \cdot \mathrm{f}(\theta_\mathrm{k}) - \mathrm{f}(\lambda) \tag{11}$$

The sum over all *k*:s was the sum of all inputs from the previous layer ($z_{input,k}$) multiplied by each individual weight θ_k, which were also mapped onto the complex state space (eq. 10). A threshold value $f(\lambda)$ was subtracted to adjust the neuron to some operating level. λ

was determined during training. After the phase rotation, the neuron's phase angle was adjusted roughly from the phase rotation by:

$$y = \frac{\pi}{2} \cdot g(\delta) - \arg(u), \tag{12}$$

where *g* was the sigmoid function, δ was a reversal parameter and *arg*() was the argument (phase angle) of the complex value u. The reversal parameter determines how (eq. 12) adjusts the phase angle of u to a real valued angle. The obtained value y was then converted back to a phase state through:

$$z_{hidden} = f(y) \tag{13}$$

and z_{hidden} was fed to the next layer as an input. The neurons in the output layer performed the same function as those in the hidden layer (eq. 11-13), but in addition, the output was converted back to a real value between [0,1]:

$$output = |Im(z)|^2 \tag{14}$$

The network was trained by back propagation with gradient descent, which calculates the error E between network output and desired output for each time step:

$$E = \frac{1}{2}\sum_t^T (desired\ output - output)^2 \tag{15}$$

The sum over t is the sum over all the points of the predicted signal. The desired output is the actual signal in the training set. Having calculated the error E, the adjustable parameters of each neuron, the weights θ_k, the threshold λ, and the reversal parameter δ, were adjusted according to the gradient descent back propagation:

$$\begin{aligned} \theta_k^{new} &= \theta_k^{old} - \eta \frac{\partial E}{\partial \theta_k}, \\ \lambda^{new} &= \lambda^{old} - \eta \frac{\partial E}{\partial \lambda}, \\ \delta^{new} &= \delta^{old} - \eta \frac{\partial E}{\partial \lambda} \end{aligned} \tag{16}$$

η is the learning rate, a value usually between 0.1 and 0.8, that determines how strongly the new value is affected by the partial derivative. A higher learning rate causes the network to fluctuate more, and longer, before reaching a desired error level, but it also ensures that the network parameter space is explored more thoroughly. A lower learning rate allows the network to approach optimal performance faster than a higher η does, but it involves the risk of the network converging to a local, but non-optimal, minimum as only a small part of the parameter space is explored. We chose η = 0.6 to allow large exploratory learning by the QNN because steering wheel signals have a transient nature.

2.4.3.6 Predicting steering (Aim 3)

To predict lane departures we first used the QNN to predict steering, and then used the transfer function to derive the lane position signals (section 2.4.3.1). We down sampled the steering wheel signals to 10 Hz, because the QNNs require even sampling frequency and because it reduces computational cost.

Our training set comprised data recorded with n=15 drivers in the night-time condition and 1265 km, or 15 % of the 8432 km of straightaway driving from all drives. For each of the 15 drivers we randomly chose driving sessions and straightaways to cover 15% of the total amount of data (evenly distributed between driving sessions and straightaways). With the training set and supervised training of the QNN we determined the parameters of each neuron in the network (eqs. 15, 16): weights θ_k, threshold λ, and reversal parameter δ.

Our test set comprised 7167 km (all straightaway data that was not used in the training set). We used 15 previous time steps, i.e. 1.5 sec of driving, to predict the next one (eqs. 9-14). We chose 15 previous time steps because it was a fairly small number of data points that still worked well when we predicted a sinusoidal "dummy signal" with 10 Hz sampling frequency. To test how well the QNN predicted the steering wheel signal, we computed the total root-mean-square error (RMSE) for all predicted signals and also for each driver and each driver as a function of time awake. The RMSE is the average error between the predictions and the measured signals.

With the predicted steering wheel signal at hand, we fed it into the simulators' transfer functions to derive the lane position signals (section 2.4.3.1).

2.4.4 Predicting lane departures from eyelid movements

For our analyses we used signals that passed our signal quality control (section 2.3.4.1). The AntiSleep software provided the parameters: average eyelid opening, blink frequency, peak closing velocity, and blink amplitude.To determine which parameter worked best, we correlated the parameters with the lane departures. For further analyses we chose the parameter with the highest correlation (Fig. 12).

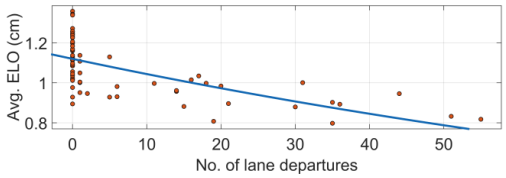

Fig. 12. Correlation between average eyelid opening and number of lane departures during a driving session (r^2 = 0.43). Data are averages across drivers (n=34).

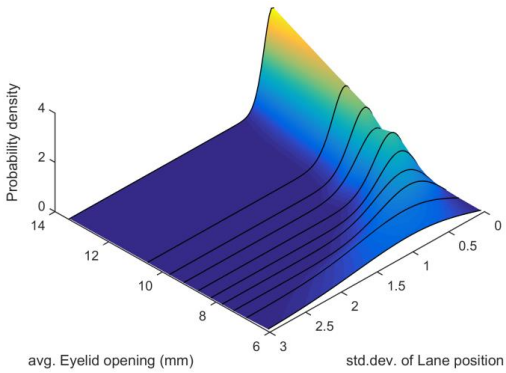

Fig. 13. Probability distribution of STDLP as a function of average eyelid opening in dark driving conditions. E.g., when the eyelid opening is 14 mm the probability that STDLP is between 0 and 50 cm is high, whereas it is low if the eyelid opening is merely 6 mm.

To predict lane departures from eyelid movements we took a Bayesian approach. First, we chose the standard deviation of lane position (STDLP) as variable to predict and average eyelid opening as predictor. Next, we estimated a probability distribution for the predicted variable given a certain condition or state of the predictor, by sampling average eyelid opening and STDLP across the whole dataset. We analyzed the driving conditions (night-time, daytime) separately. We split each driving session into 2.5 minute bins (24 bins per session). For each bin, we computed a sample pair of average eyelid opening and STDLP. We sorted the samples by increasing average eyelid opening, and generated a surface by fitting a Rayleigh distribution to the STDLP and eyelid opening data. Finally we interpolated between the distributions. Figure 13 shows the derived state space.

3. RESULTS AND DISCUSSION

3.1 Objective sleepiness and simulator sickness

Figure 14 shows how objective sleepiness evolved during the 36-hour experiment. The number of lapses on the objective PVT was consistently higher for drivers that drove in the night time condition (Table 3). The number of lapses increased during the experiment (Table 3) but not after a drive (Table 3). Taken together, these results show that the study protocol implemented in Työtehoseura's facilities was scientifically sound.

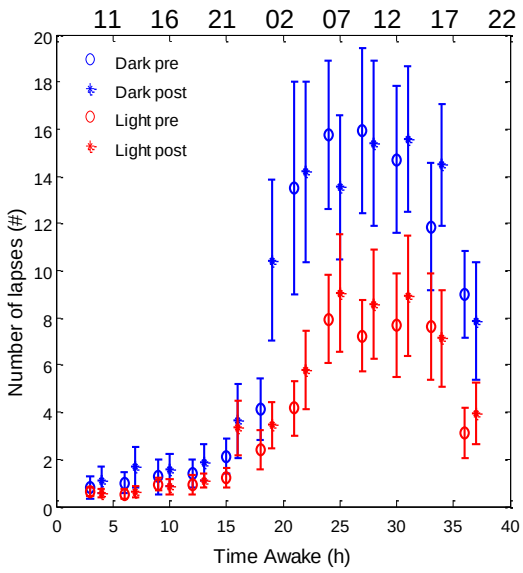

Fig. 14. Objective sleepiness as a function of time awake (lower x-axis) and time of day (upper x-axis) for drivers in the night time condition (blue) and daytime condition (red), both before (open circles) and after (asterisks) drive. Mean ± SEM.

Figure 15 shows how the symptoms of nausea, oculomotor strain, disorientation, and total scores in the simulator sickness questionnaire evolved during the 36-hour experiment. The light condition did not affect how the drivers rated their symptoms or the total score (Table 3). However, all symptoms and the total score increased during the experiment (Table 3). The (group- level) disorientation and total scores increased after the drives (Table 3).

Post hoc analysis of the first six driving sessions showed that the (group-level) disorientation scores had increased after the second ($F_{1,63}$=3.09, p=0.08) and third ($F_{1,63}$=4.54, p=0.04) sessions. To identify which drivers contributed to this increase, we plotted the total scores of each driver as a function of driving session as well as the pre-post measurements. Ten (n=10) drivers exhibited increased total scores after the first driving session, n=12 drivers after the second session, and n=10 drivers after the third session.

Table 3. Effect of light condition, sleep loss, and time on task on markers of sleepiness and simulator sickness. Light condition: night versus day; Driving session: from 1 to 12; Pre- post: scores before and after driving.

Measurement	Light condition	Driving session	Pre- post
PVT	$F_{1,734}$=25.1 (**p<0.001**)	$F_{11,734}$=36.3 (**p<0.001**)	$F_{1,734}$=2.31 (**p<0.001**)
Nausea	$F_{1,734}$=0.55 (p=0.46)	$F_{11,734}$=51.1 (**p<0.001**)	$F_{1,734}$=2.64 (p=0.11)
Oculomotor	$F_{1,734}$=0.26 (p=0.61)	$F_{11,734}$=98.4 (**p<0.001**)	$F_{1,734}$=2.77 (p=0.10)
Disorientation	$F_{1,734}$=0.11 (p=0.74)	$F_{11,734}$=36.4 (**p<0.001**)	$F_{1,734}$=4.72 (**p=0.03**)
Total Score	$F_{1,734}$=0.06 (p=0.82)	$F_{11,734}$=59.3 (**p<0.001**)	$F_{1,734}$=5.18 (**p=0.02**)

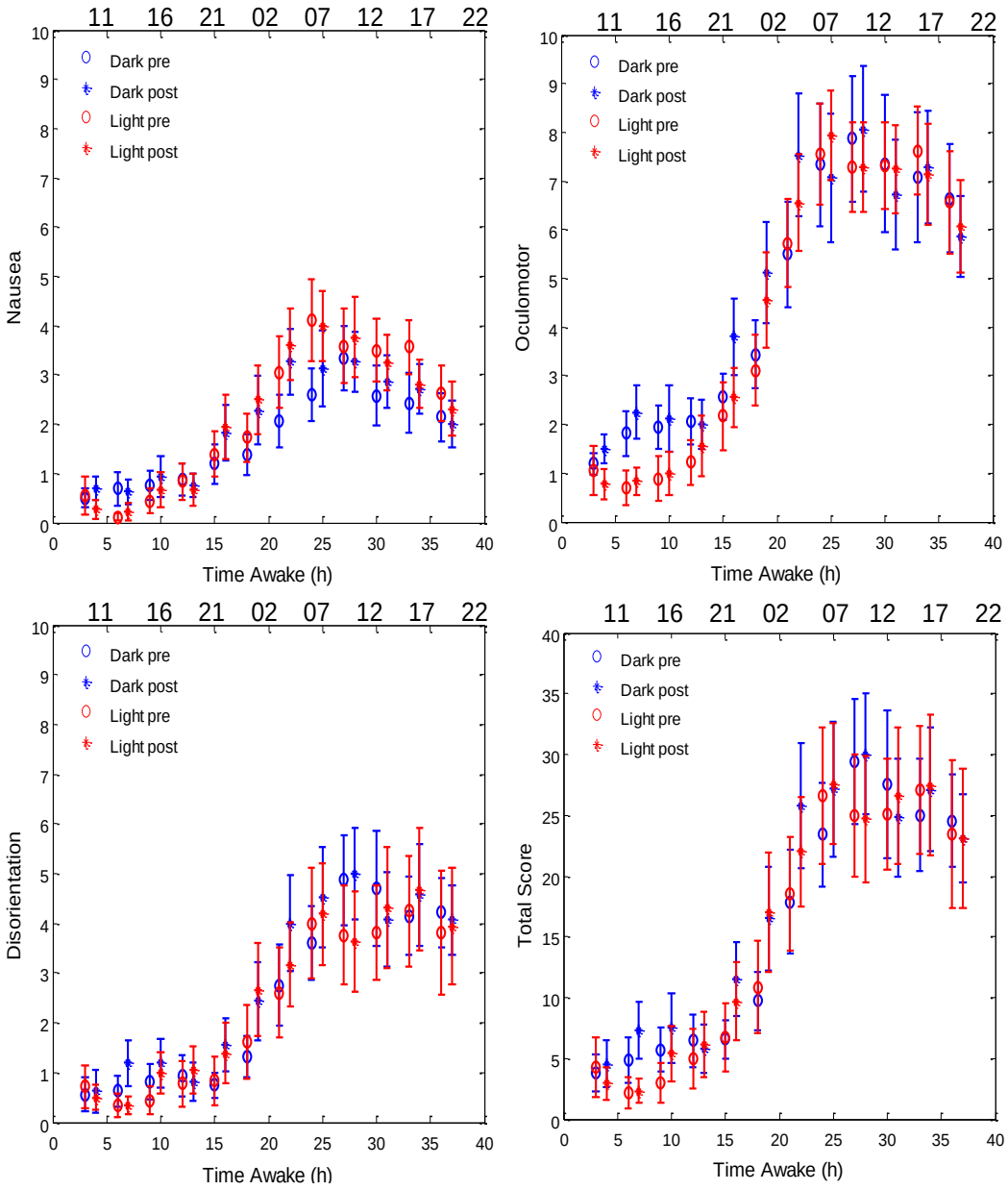

Fig. 15. Symptoms of nausea (in a), oculomotor strain (in b), disorientation (in c), and total score in the simulator sickness questionnaire. Axes and legends as in fig. 14. Mean ± SEM.

3.2 Predicting simulator sickness from HRV (Aim 1)

Figure 16 shows the HRV parameters HF power and LF/HF ratio in the drivers whose SSQ total scores had increased after the 1st, 2nd, or 3rd driving session ("Increase in SSQ") and in the rest of the drivers ("control"). Before the driving sessions, the LF/HF ratio was lower in the "Increase in SSQ" group than in the "Control" group. However, the pre- drive difference between the groups did not reach statistical significance.

The lack of predictive power (pre- drive data in Fig. 16) and lack of correlation between the HRV parameters and our gold standard (not shown) probably stems from the fact that overall, the participants in our study did pretty well. The four drivers that aborted the sleep deprivation experiment did not give simulator sickness as the reason for quitting. In fact, none of the n=34 participants reported feeling simulator sick at any point, not even during the training session on Monday, which was unexpected.

One explanation could be that none of the participants were prone to simulator sickness. The fact that they were students at Työtehoseura's branch of vehicles and logistics means

that they had driven in the simulators before. Perhaps they would not have volunteered for the study in the first place if they had been aware of a tendency towards simulator sickness. Another explanation could be that the highway scenarios they drove in did not promote simulator sickness. Driving in a night-time scenario does not challenge the driver's sensory systems with as much conflicting information as driving in a daytime scenario does. Nevertheless, adding light to the highway scenario did not induce simulator sickness in the participants (Fig. 15 and Table 3).

Overall, the SSQ total score was low during the first three sessions when the drivers still felt rested (Fig. 15). Nevertheless, the pre-drive LF/HF ratio was lower in the "Increase in SSQ" group than in the "Control" group. This difference (although not statistically significant) is important – since the parameter reacted to a modest increase in simulator sickness it may mean that a person with more pronounced tendency to simulator sickness the parameter could actually be a sensitive predictor for onset of simulator sickness symptoms. This should be examined with volunteers who are prone to simulator sickness. If found that the LF/HF ratio does predict an increase in SSQ scores with participants who clearly express simulator sickness, it should be straightforward to implement the method in practice. The skin electrodes we used may not be necessary, a heart rate belt may suffice. Moreover, the eMotion Faros 180° could transmit data in online mode directly to a computer with analysis software. This would allow the instructor to catch students whose pre-drive LF/HF ratio is lower than a predefined threshold.

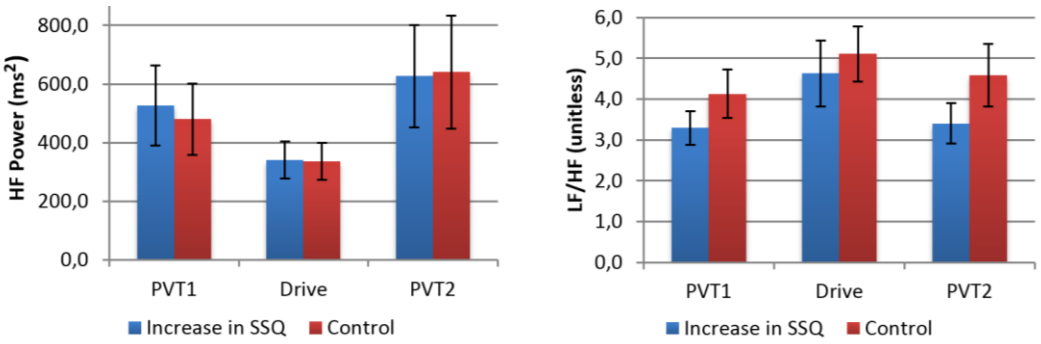

Fig. 16. HF power (left) and LF/HF ratio (right) in control drivers and drivers with increased SSQ after the driving sessions. Data are averages across test sessions 1 to 3. PVT1 indicates pre- drive data. Mean ± SEM.

3.3 Deriving lane position from steering (Aim 2)

A transfer function with model order m=8 rendered the highest correlation between the derived and measured lane position signals. For simulator #1, the transfer function (eq. 2) was:

$$TF_8 = \frac{-1.006+2.497s-16.53s^2+14.6s^3-57.96s^4+13.57s^5-51.74s^6}{0.0142+7.808s+29.42s^2+326.4s^3+388.2s^4+2188s^5+630.3s^6+2853s^7+1s^8}, \quad (17)$$

and for simulator #2, it was:

$$TF_8 = \frac{3.953-22.11s+46.31s^2-117.1s^3+41.83s^4-94.14s^5+21.2s^6}{0.0401+21.13s+173.1s^2+3961s^3+4574s^4+22500s^5+10790s^6+19500s^7+1s^8}. \quad (18)$$

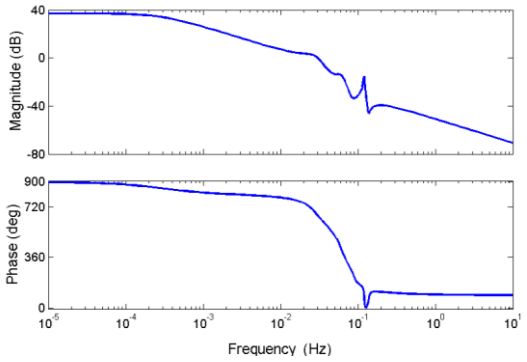

Fig. 17. Simulator transfer function between steering wheel angle and lateral lane position for simulator #1.

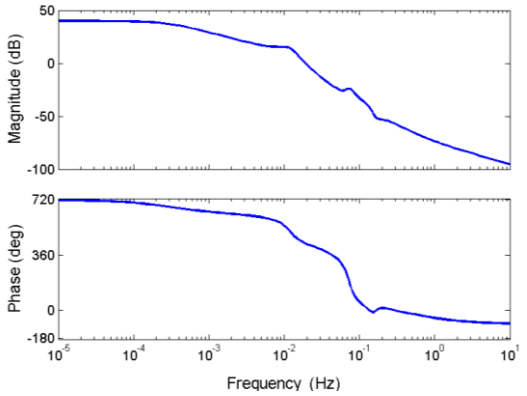

Fig. 18. Simulator transfer function between steering wheel angle and lateral lane position for simulator #2

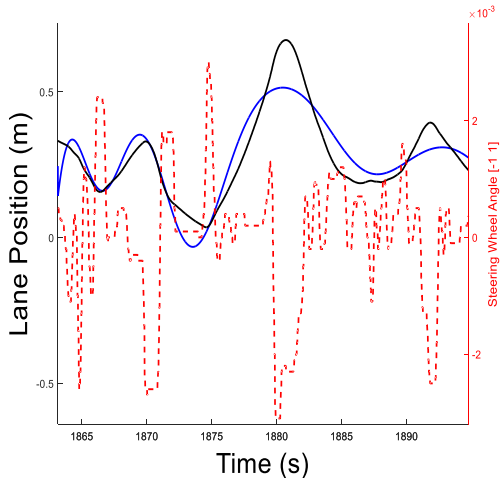

Fig. 19. Actual lane position (black), steering wheel signal (red), and derived lane position (dashed blue) for one 0.7-km straightaway during the 1st driving session in the night condition (simulator #2). The correlation between actual and derived lane position was r=0.57.

Both simulators worked as amplifying low pass filters with the cut-off frequencies 0.31 mHz (simulator #1) and 0.36 mHz (simulator #2)(Fig. 17-18). Figure 19 illustrates the correlations between measured and derived lane position signals. In the validation set, the average Pearson correlation between actual and derived lane position signals was r=0.21 (n=17, simulator #1) and r=0.27 (n=18, simulator #2). In the test set, the average Pearson correlation between actual and derived lane position signals was r=0.43 (simulator #1) and r=0.48 (simulator #2) (Fig. 20-21).

Visual inspection of the actual and derived lane position signals showed that the correlation between them was high in the beginning of the straightaways but decreased after the first 30 seconds (Fig. 19). At 80 km/h, the car covers 670 m in 30 seconds.

Taken together this shows that one can derive the lane position signal from the steering wheel signal with the simulator's transfer function, which con firms our previous finding [9]. However, the transfer function was developed for a linear system and therefore it works well only when applied to signals shorter than 30 seconds. Next, we should develop the method for a non-linear system.

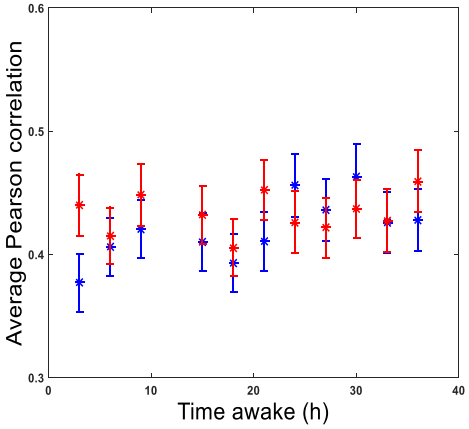

Fig. 20. Average correlation coefficients between the actual and derived lane position of the test set as a function of time awake (simulator #1) for drivers in daylight (red) and nighttime (blue) conditions. The correlation across all data points is r=0.43. Mean ± SEM.

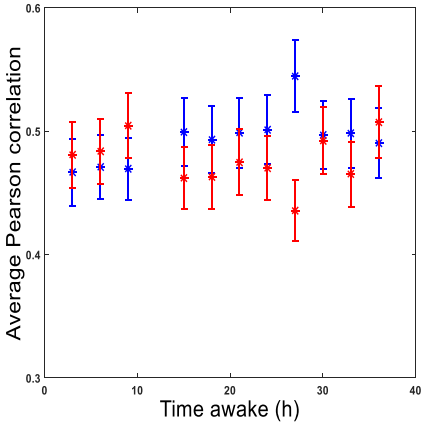

Fig. 21. Average correlation coefficients between the actual and derived lane position of the entire test set as a function of time awake (simulator #2) for drivers in daylight (red) and nighttime (blue) conditions. The correlation across all data points is r=0.48. Mean ± SEM.

3.4 Detecting lane departure from steering (Aim 2)

Figure 22 illustrates the performance of the lane departure detection algorithm. It detected lane departures from the derived lane position signal before they occurred in the measured signal, but also failed to issue warnings, and also gave false warnings.Table 4 shows the sensitivity and specificity of the algorithm as a function of the time it allows the vehicle to drive outside the lane before it issues a warning. Issuing a warning after 1 s results in slightly higher sensitivity than using a longer time windows. The rationale is that many of the lane departures were shorter and would not be detected with a longer window.

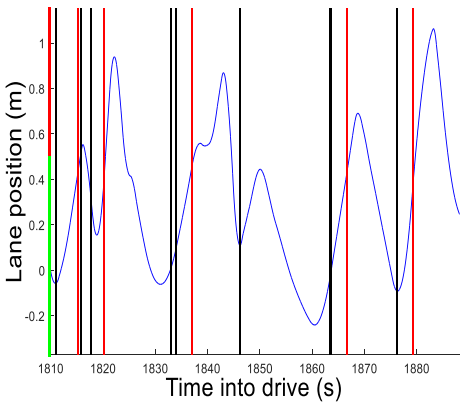

Fig 22. Lane departure warnings. Red lines indicate actual lane departures. Black lines indicate issued warnings. In the middle of the straightaway there was a false warning. Y-axis is divided into 'safe zone' (-0.5<x<0.5 m, green) and 'danger zone' (x>0.5 m, red).

Table 4. Sensitivity and specificity of LDW algorithms with different time windows allowed outside the lane before a warning is issued.

Time window (s)	Sensitivity (%)	Specificity (%)
1	0.4706	0.7077
2	0.4665	0.7063
3	0.4615	0.7085
4	0.4636	0.7110
5	0.4611	0.7152

Our success criterion was to derive lane position signals that correlated with the measured lane position signal with $r \geq 0.78$ [9]. While the achieved correlation was lower than that, the other success criterion was met. The sensitivity 47% was higher than that of current video-based LDW systems, 40% [8].

Taken together this means that one can detect lane departures from the steering wheel signal. While the transfer function is vehicle-specific, this function can be determined during a test drive. Next, we should test whether the proposed LDW system is field-capable.

3.5 Predicting lane departures from steering (Aim 3)

Our QNN comprised 1542 parameters that we optimized for the training set data.

Ee applied the trained QNN on the test set, predicted the steering wheel signal one time step ahead, and computed the root-mean-square error between the QNN output and the actual steering wheel signal. The RMSE was fairly stable both across the drivers (Fig. 23) and across their time awake (Fig. 24). The QNN's ability to predict the steering wheel signal did not depend on driver or his/her time awake. Hence, the parameters that we determined in the training set should work well on new drives. On average, across all drivers, the error was RMSE=0.007±0.004 (mean ± SD). This corresponds to 0.7% (the steering wheel signal was scaled to the range [0,1]). Often the desirable error level during training is at most 1%, so our QNN performed in line with this Then again, on straighta-ways the steering wheel usually varied between [-0.01,0.01].

Visual inspection of the actual and predicted steering wheel signals revealed that the main contributor to the prediction error was an offset between the baseline levels of the signals (Fig. 25). For example, in Fig. 25, the offset[1] was 0.005, which means that most of the error stems from this offset. In some signals, atypical events, which the QNN couldn't handle, were present (Fig. 26). However, after the atypical events the QNN resumed predicting with previous performance.

Our hypothesis was that we could use QNNs to predict lane departures from steering. However, this did not work, because the QNN perceived the lane position signal as a constant bias – the variations in the lane position signal were much slower than the variations in the steering wheel signal. Scaling the lane position signal to a suitable range for the QNN would have precluded the QNN from predicting large lane departure (as the output would have been restricted to some range). Therefore, our second approach was to use the predicted steering wheel signals as inputs to the transfer function based approach to derive lane position (section 2.4.3.1). Figure 27 shows an example.

Taken together we showed that QNNs can predict the steering wheel signal one time step ahead (in our case equaling 0.1 sec). Combined with lane departure detection it contributes towards prediction of lane departures. To our knowledge, other researchers have used QNNs to predict one time step ahead [15, 25-27]. For the purpose of traffic safety our next step will be to train the QNN to predict several time steps ahead. One approach could be to use the predicted datapoints as inputs in the QNN input layer. Figure 28 shows an example with our currently trained QNN: after 20 time steps the predicted signal starts to diverge[2]. Another approach, which is computationally heavy, could be to train the network to predict several time steps ahead.

[1] The offset stems from different drivers making different steering movements and from the two different simulators in the study – the combined effect on the network manifests as an offset. It could be thought of as some average in zero level between all the drivers in the training set.

[2] How fast the predicted signal starts diverging depends on how sudden the changes in the topical signal portion are – the closer the starting point is to a transient, the faster the predicted signal will diverge.

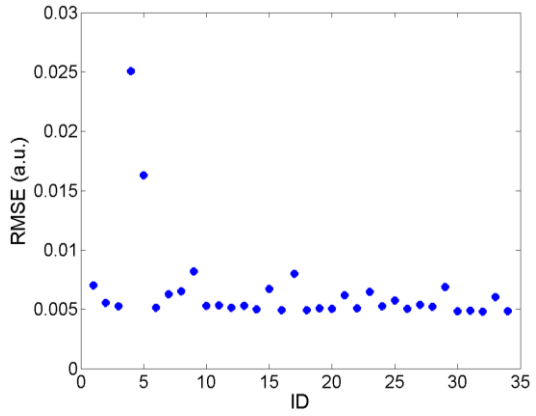

Fig. 23. QNN performance when predicting 1 time step ahead. RMSE as a function of driver ID. RMSE has steering wheel signal units. There was no difference between simulator #1 and simulator #2 or between the night (ID 1-16) and day conditions (ID 17-34).

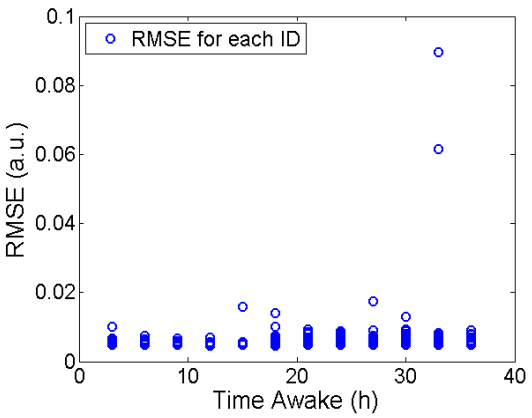

Fig. 24. QNN performance when predicting 1 time step ahead. RMSE for each driver as a function of time awake. Each circle is one driver at a specific time awake. RMSE is in the units of the steering wheel signal.

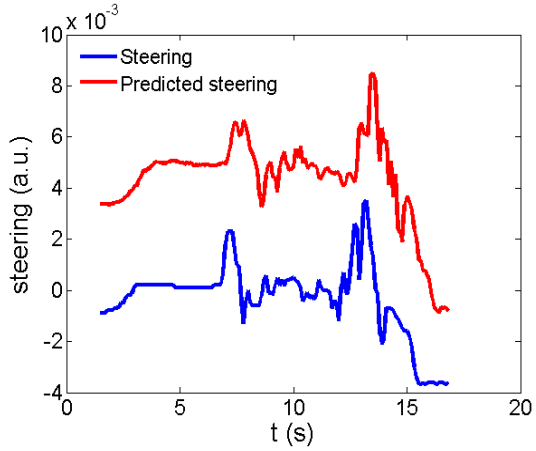

Fig. 25. Actual (blue) and predicted (red) steering wheel signal (when predicting 1 time step ahead): with no atypical events in the actual steering wheel signal the RMSE between actual and predicted signal is small (in this example RMSE is 0.005 This signal was recorded at 18 h time awake.

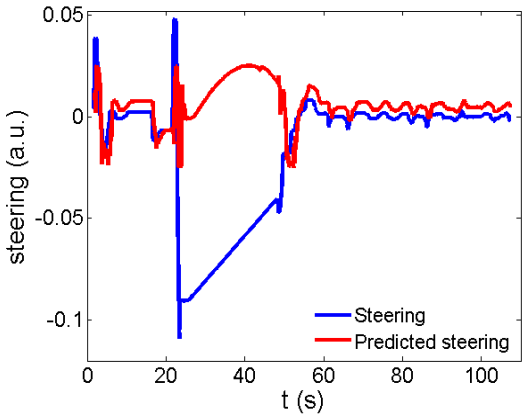

Fig. 26. Actual (blue) and predicted (red) steering wheel signal (when predicting 1 time step ahead): the QNN predicts poorly during the atypical event (20 - 50 s) but recovers after the event with the same performance as before it (in this example RMSE is 0.042). This signal was recorded at 30 h time awake.

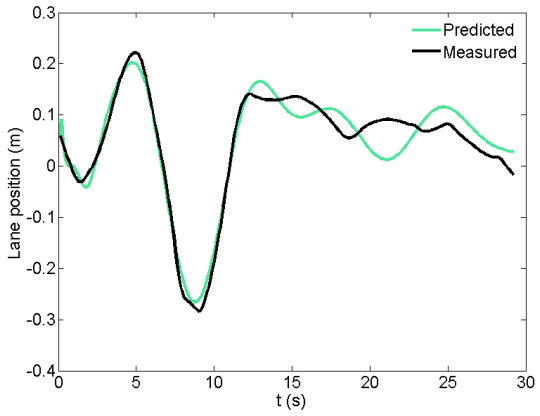

Fig. 27. Measured lane position signal (green) and derived lane position signal The correlation was r=0.73.

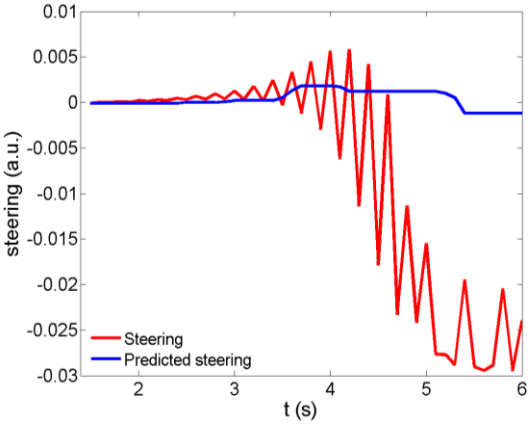

Fig. 28. Predicted values, corrected for the offset, was fed to the QNN as inputs. The predicted values starts diverging after approximately 20 time steps (2 s). Time awake was 3 h.

4 CONCLUSIONS

We provided the first results that a lower ratio between the low- and high frequency components in the heart rate variability precedes a small increase in the scores on the Simulator Sickness Questionnaire. This finding was based on a group of people with no pronounced simulator sickness, so before any firm conclusions can be drawn, we need to replicate the results with volunteers who clearly express simulator sickness.

We developed an algorithm that detects lane departures from the steering wheel signal with higher sensitivity than the current video-based systems do. Our next task is to increase the sensitivity even more. Because the method was developed from data recorded in a laboratory-environment we also need to test whether it works in the field. If it does, we have provided road transportation with the first lane departure warning (LDW) system that is based on a robust in-car signal.

Finally, we showed that Quantum Neural Networks can predict the steering wheel angle 0.1 s ahead with 0.35% error (i.e., high accuracy) and that the predicted signal can be used to derive the lane position signal. If we can increase the predicttion horizon we have the necessary elements for a predictive in-car LDW system.

5 ACKNOWLEDGMENT

This work was funded by the Finnish Work Environment Fund. We would also like to extend our sincerest thanks to Mr. Aarno Lybeck, Business Director at Työtehoseura Logistics and Vehicles, for facilitating seamless collaboration between our teams; to Mr. Mikko Rautio for recruiting the study participants, for helping us to implement the measurements in Työtehoseura's facilities, and for operating the simulators during the measurements; to Mr. Arto Kyytinen for helping us to set up the gadget synchronization; to rest of the staff at Työtehoseura who operated the simulators during the measurements; to Mr. Eero Pajarre, CEO at Eepsoft Oy, for customizing the simulator software that recorded data from the simulators. Finally, thank you to all study participants for enduring the sleep deprivation experiments!

References

1. *Evaluation of US Department of Transportation Efforts in the 1990s to Address Operator Fatigue*, in National Transportation Safety Board, Safety Report NTSB/SR-99/01, Washington DC 1999.
2. VALT, *Yearly Report of Road Accidents with Killed Occupants Studied by Road Accident Investigation Teams in 2001* (In Finnish). Helsinki: Finnish Motor Insurers' Center 2006.
3. Häkkänen H, Summala H. *Sleepiness at work among commercial truck drivers*. Sleep 2000;23(1):49-57.
4. Thiffault P, Bergeron J. *Monotony of road environment and driver fatigue: a simulator study*. Accid Anal Prev 2003;35(3):381-391.
5. Verwey WB, Zaidel DM. *Preventing drowsiness accidents by an alertness maintenance device*. Accid Anal Prev 1999;31(3):199-211.
6. Philip P, et al. *Fatigue, alcohol, and serious road crashes in France: factorial study of national data*. Bmj 2001;322(7290):829-830.
7. Sagaspe P, et al. Extended *driving impairs nocturnal driving performances*. PLoS One 2008;3(10):e3493.
8. Fröberg PÅ. *Volvo Cars introduces new systems for alerting tired and unconcentrated drivers*, Press Information 2007-08-28, Volvo Car Corporation (Retrieved on 22.1.2013).
9. Forsman PM, et al. *Efficient driver drowsiness detection at moderate levels of drowsiness*. Accid Anal Prev 2013;50:341-350.
10. Highway Loss Data Institute, Status Report, Special issue: crash avoidance, 2012;47:5(3).
11. Alkim TP, et al. *Field Operational Test "The Assisted Driver"*. IEEE Intell Vehic Symp 2007;p. 1198-1203.
12. Vadeby A, et al. *Sleepiness and prediction of driver impairment in simulator studies using a Cox proportional hazard approach*. Accid Anal Prev 2010;42(3):835-841.
13. Ferreira TAE et al. *A new intelligent system methodology for time series forecasting with artificial neural networks*. Neur Proc Letters 2008;28(2):113-129.
14. Araújo RA. *A robust automatic phase-adjustment method for financial forecasting*. Knowldge-Based Systems, 2012;27:245-261.
15. Hui S, et al. *A hybrid time lagged network for predicting stock prices*. International Journal of the Computer, the Internet and Management, 2000;8:26-40.
16. Goode N, et al. *Simulation-based driver and vehicle crew training: Applications, efficacy and future directions*. Appl Erg 2013;44:435-444.
17. Brooks JO, et al. *Simulator sickness during driving simulation studies*. Accid Anal Prev 2010;42:788-796.
18. Cobb SVG, et al. *Virtual reality-induced symptoms and effects (VRISE)*. Presence 1999;8(2):169-186.
19. Åkerstedt T, Gillberg M. *Subjective and objective sleepiness in the active individual*. Int J Neur 1990;52:29-37.
20. Basner M, Dinges D. *Maximizing sensitivity of the psychomotor vigilance test (PVT) to sleep loss*. Sleep 2011;34(5): 581.
21. Kennedy RS, et al. *Simulator sickness questionnaire: an enhanced method for quantifying simulator sickness*. Int J Aviat Psyc 1993;3(3):203-220.
22. Van Dongen H et al. *The cumulative cost of additional wakefulness: dose-response effects on neurobehavioral functions and sleep physiology from chronic sleep restriction and total sleep deprivation*. Sleep 2003;26(2):117-129.
23. Lyzell C. *Initialization Methods for System Identification.* Division of Automatic Control Department of Electrical Engineering Linköping University, Linköping 2009
24. Björck A. *Numerical methods for least squares problems.* SIAM, Philadelphia 1996
25. Kouda N et al. *Qubit neural network and its learning efficiency.* Neural Computing & Applications, 2005;14:114-121.
26. Li X et al, *A study on sunspot number time series prediction using quantum neural networks* in *Genetic and Evolutionary Computing, 2008. WGEC'08. Second International Conference on*, 2008, pp. 480-483.
27. Mahajan R. *Hybrid quantum inspired neural model for commodity price prediction*, in *Advanced Communication Technology (ICACT), 2011 13th International Conference on*, 2011, pp. 1353-1357.
28. Friedrichs F and Yang B. *Drowsiness monitoring by steering and lane data based features under real driving conditions.* 18th European Signal Processing Conference (EUSIPCO-2010), Aalborg 2010
29. Tarvainen et al., *Kubios HRV – Heart rate variability analysis software*, Computer Methods and Programs in Biomedicine, 2014;113(1):210-220.
30. Task Force of The European Society of Cardiology and The North American Society of Pacing and Electrophysiology, Heart rate variability Standards of measurement, physiological interpretation, and clinical use. European Heart Journal, 1996;17:354–381.

HELSINGIN YLIOPISTO
HELSINGFORS UNIVERSITET
UNIVERSITY OF HELSINKI